Available online at www.sciencedirect.com
ScienceDirect
Tetrahedron
Tetrahedron 62 (2006) 10434–10440

Cell penetrating silica nanoparticles doped with two-photon absorbing fluorophores

Loris Bertazza,[a] Lucia Celotti,[a] Graziano Fabbrini,[b] Maria Antonietta Loi,[c,d] Michele Maggini,[b] Fabrizio Mancin,[b,*] Silvia Marcuz,[b] Enzo Menna,[b] Michele Muccini[c] and Umberto Tonellato[b]

[a]*Dipartimento di Biologia, Università of Padova, via Bassi 58B, I-35121 Padova, Italy*
[b]*Dipartimento di Scienze Chimiche, Università of Padova, via Marzolo 1, I-35131 Padova, Italy*
[c]*CNR, Istituto per lo Studio dei Materiali Nanostrutturati, via Gobetti 101, I-40129 Bologna, Italy*
[d]*Physics of Organic Semiconductors, Materials Science Centre, University of Groningen, Nijenborgh 4, 9747 AG Groningen, The Netherlands*

Received 9 June 2006; revised 28 July 2006; accepted 11 August 2006
Available online 7 September 2006

Abstract—Organosilica nanoparticles, doped with two-photon absorbing distyrylbenzene derivatives, were prepared and studied as cell staining agents. Two dyes were used, bearing either two peripheral dimethylamino groups or one dimethylamino and one cyano group. Due to the internal charge transfer character of their excited state, the dyes employed show a red-shifted quenched emission in polar solvents. Once included in the particles, the properties of the two dyes undergo a substantial variation. Particles doped with the cyano substituted distyrylbenzene show a remarkable emission quantum yield in water, probably due to solvent exclusion from the nanoparticle core. To the contrary, the emission of the particles containing the dye substituted with two dimethylamino groups is substantially quenched. Fluorescence emission induced by two-photon absorption follows the same behaviour. The doped nanoparticles can be rapidly internalized by tumour cells with accumulation limited to the cytoplasm and show no cytotoxicity at low concentrations.

1. Introduction

The synthetic procedure to prepare nearly monodisperse silica nanoparticles by condensation of tetralkoxysilanes is known since the late '60s from the work of Stöber.[1] Later on, several modifications of this procedure have been proposed to prepare dye-doped silica nanoparticles (DDNs).[2] Such materials have been attracting an increasing interest in the last years for their potential applications in biology, medicine and as sensors. DDNs are easy to prepare, cheap, water soluble and provide several compartments (bulk, surface, mesopores, shells, etc.) that can be conveniently engineered to perform different functions. As a consequence, DDNs are used to stain cells,[2b,3] in immunoassays,[4] as traceable vectors capable of delivering drugs[2c,5] or DNA[6] within cells and as scaffolds for the realization of complex fluorescent nanosensors.[7]

Among the great variety of dyes available for inclusion in functional nanostructures, two-photon absorbing (TPA) fluorescent dyes have gained increasing relevance for applications in the bio-imaging field.[8] TPA bio-imaging is a non-invasive, non-destructive technique that employs near IR light (usually in the 700–1000 nm range), which is not absorbed by biological tissues, as pumping source. Another advantage is that TPA-induced fluorescence allows a better 3D spatial resolution than other imaging methods based on one-photon processes, as the non-linear nature of the TPA phenomenon limits the emitting sample volume to the close vicinity of the focal point of the IR laser beam.[9] Moreover, the use of long wavelength light allows deeper penetration of the tissues and low scattering of the excitation beam. Many research efforts are focusing on the development of chromophores with large TPA cross sections in order to allow the use of low laser intensities.[10] Most of these chromophores are, however, complex molecular structures that are often insoluble in water and require multistep syntheses.

DDNs are a valuable alternative to pristine dyes. In fact, a single particle can be loaded with several dye molecules with an overall improvement of absorptivity and emission characteristics of these systems, when compared to those of isolated molecules.[2b,11] Furthermore, inclusion of the dye in the particle could overcome possible solubility problems of the dye itself, while surface functionalization can give the DDN assembly a cell penetrating ability and even specificity.[2–6,12] The toxicity of the dye to the host organism should be minimized since the fluorophore is not released from the particle. Finally, segregation from the solvent, if

Keywords: Silica nanoparticles; Two-photon absorption; Fluorescent dyes; Cellular uptake.
* Corresponding author. Tel.: +39 0498275666; fax: +39 0498275239; e-mail: fabrizio.mancin@unipd.it

0040–4020/$ - see front matter © 2006 Elsevier Ltd. All rights reserved.
doi:10.1016/j.tet.2006.08.044

effective, could lead to other advantages such as decreased photobleaching and solvent quenching of the emission.[2b] Besides such advantages, the use of DDNs could present problems, such as dye aggregation within the particles, giving rise to concentration self-quenching of the emission, or particle toxicity.

Examples of silica nanoparticles doped with fluorescent dyes optimized for two-photon absorption are however quite scarce. Prasad and co-workers anchored a thiol modified hemicyanine dye either to ZnS[2c] or Fe_2O_3[12] nanoparticles and coated them with a silica shell. Recently, the same authors included a naphthalenylvinylpyridine derivative modified with a trialkoxysilane moiety into silica particles, obtaining a ratiometric pH fluorescent probe.[7g] In this paper we describe the preparation and properties of organosilica nanoparticles doped with TPA fluorophores of the distyrylbenzene (DSB) class, and their cell permeation ability.

2. Results and discussion

2.1. Synthesis and properties of the dyes

The DSB molecular structure was selected as its derivatives are known to have good two-photon cross sections and noticeable fluorescence quantum yield.[10a,13] Moreover, the synthesis of DSB derivatives is quite straightforward under Wittig or Wadsworth–Emmons coupling conditions. Compounds **1** and **2** (Chart 1) were selected in order to investigate the effect of peripheral functional groups with different electronic demands. Dye **1** was prepared as reported in the literature.[14] Compound **2** was synthesized in 58% yield from phosphonate **3** and 4-(dimethylamino)benzaldehyde through a Wadsworth–Emmons coupling reaction (Scheme 1).

Absorption spectra of **1** and **2**, typical of substituted DSB derivatives,[15] are reported in Figure 1. They show a strong absorption band at about 400–420 nm and a weaker one at 320 nm, with the maxima of **2** slightly red-shifted relative to that of **1**. The position of the absorption maxima is almost insensitive to solvent polarity with the exception of DMSO (not shown), where a 14–16 nm red shift was observed. On the contrary, the emission spectra of the two fluorophores are strongly sensitive to the solvent (Fig. 2): in both cases, as the solvent polarity increases, the spectra are red-shifted, broader and much less intense. A comparable behaviour has been already observed in similar systems and was attributed to a strong ICT (Internal Charge Transfer) character of the excited state.[15] Changing the solvent from hexane to DMSO, the fluorescence quantum yield decreases from 0.36 to 0.23 and from 0.21 to 0.04, respectively, for **1** and **2**. The effect on **2** is more evident as may be expected if one considers that the ICT character of the excited state is enhanced by the presence of the electron withdrawing cyano group.

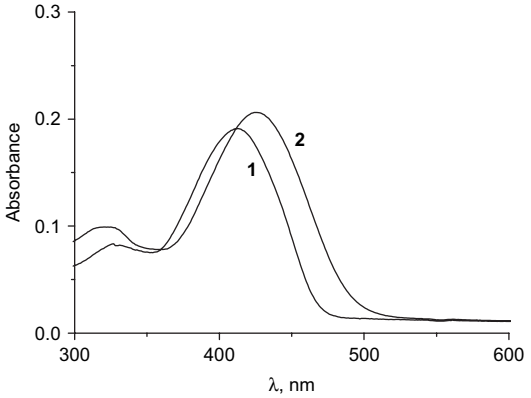

Figure 1. Absorption spectra of dyes **1** and **2** in ethanol. Selected data: [dye]=2.5×10^{-6} M, **1**: λ_{max}=413 nm ($\varepsilon=6.9\times10^4$ M^{-1} cm^{-1}), **2**: λ_{max}=425 nm ($\varepsilon=7.3\times10^4$ M^{-1} cm^{-1}).

2.2. Preparation and characterization of DDNs

The inclusion of dyes **1** and **2** into silica particles was performed following a procedure reported by Prasad and co-workers[2d] modified as follows. Propyltriethoxysilane (PTES) and 3-aminopropyltriethoxysilane (APTES) were co-polymerized in water in the presence of AOT (sodium bis(2-ethylhexyl)sulfosuccinate) micelles loaded with the dye. Polymerization of the organosilanes takes place in the non-polar core of the micellar aggregates, which also incorporate the poorly water soluble dye, and results in the formation of dye-doped organisilica (ORMOSIL) particles. This method appeared not only simple but also suitable for the preparation of DDNs since it does not require any chemical modification of the fluorophore before its incorporation in the particles.

The formation of the colloids was followed by Dynamic Light Scattering (DLS) measurements. The resulting particles were purified by extensive ultrafiltration over a 10,000 Da (~3 nm) cut-off membrane to eliminate unreacted species and hydrolyzed monomers. No dye was detected in the filtrate, thus indicating the absence of leaking from the particles, at least in the short term. Colloid dimensions and morphology were investigated using Transmission

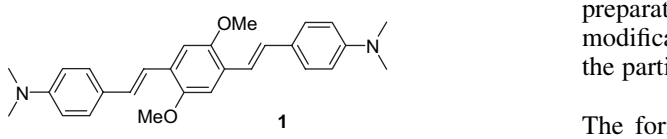

Chart 1.

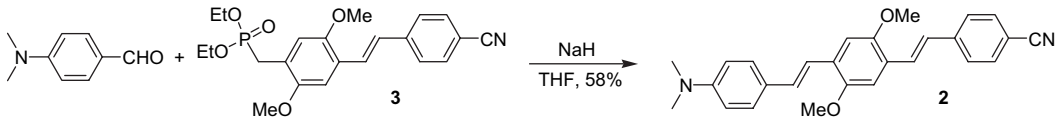

Scheme 1. Synthesis of DSB derivative **2**.

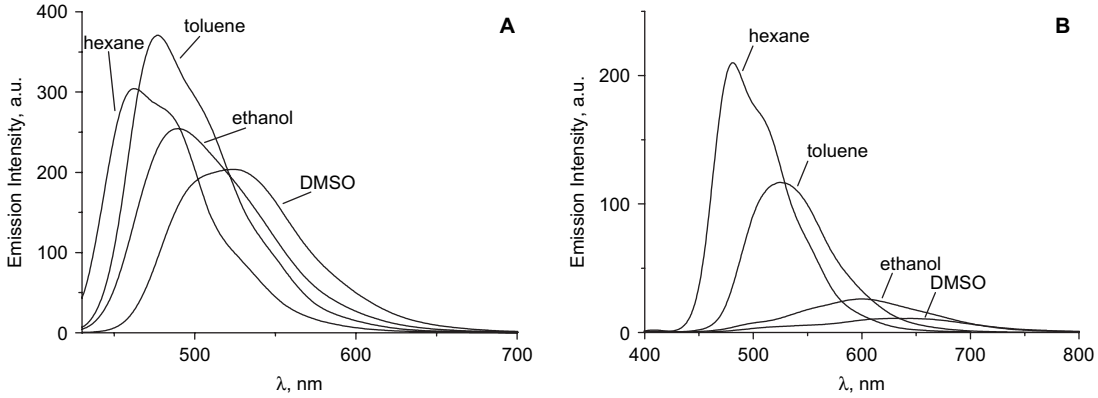

Figure 2. Emission spectra of dyes **1** (A) and **2** (B) in different solvents. Conditions: λ_{exc}=410 nm, [dye]=1.0×10^{-6} M, 25 °C.

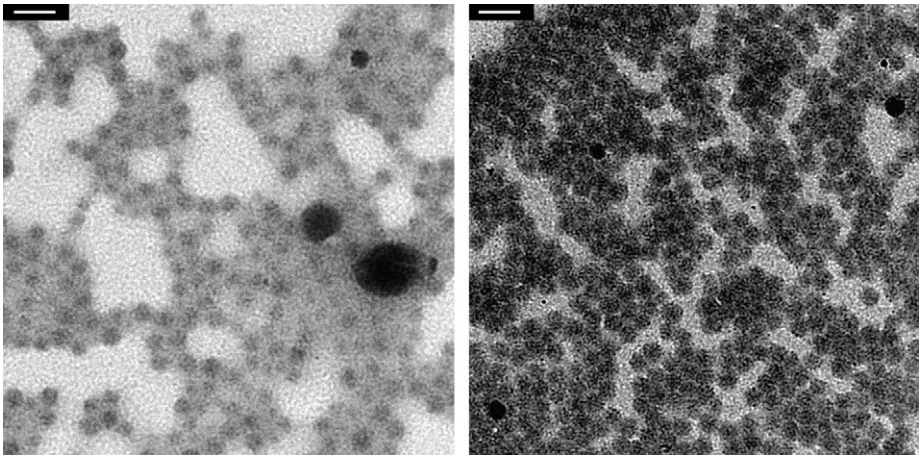

Figure 3. TEM images of dye-doped silica nanoparticles containing compounds **1** (left) and **2** (right), the bars (upper left corners) correspond to 100 nm.

Electron Microscopy (TEM, Fig. 3) and DLS (Table 1). The agreement between the hydrodynamic diameters obtained by DLS and the diameters obtained by electron microscopy is good. The particles appear spherical with a fairly low polydispersity.

The absorption spectra of DDNs in ethanol/water 9:1 are similar to those of the dyes in solution (Fig. 4). This allowed an estimation of the dye concentration in the DDN samples by absorbance measurements. On the other hand, nanoparticle concentrations (mg/mL) were determined by solvent evaporation. Typical DDN aqueous solutions, after purification, had 3.0–3.5 mg/mL nanoparticle concentration and 13–14 μM dye content.[16]

Interestingly, the spectrum of DDNs containing **1** (**1np**) in pure water shows some peculiarity (Fig. 4): the main band is blue-shifted at 392 nm and has a complex shape with several shoulders at 350, 425 and 475 nm. Such a solvent effect is not observed in the case of DDNs containing **2** (**2np**), which show similar features both in ethanol and in water (Fig. 4).

Table 1. Nanoparticles diameter (D, nm) and polydispersity (δ) of DDNs as obtained by Transmission Electron Microscopy (TEM) and Dynamic Light Scattering (DLS)

DDNs	Dye	$D_{(TEM)}$, nm	δ, nm (%)	$D_{(DLS)}$, nm
1np	**1**	28.7	7.4 (18%)	31.4
2np	**2**	38.4	6.2 (16%)	36.6

Fluorescence spectra of the DDNs in water are reported in Figure 5. Inclusion of the dyes within the particles is assessed by the high fluorescence anisotropy values recorded: 0.36 for **1np** and 0.33 for **2np**. Such values confirm the low mobility of the dyes due to grafting to the nanoparticles.

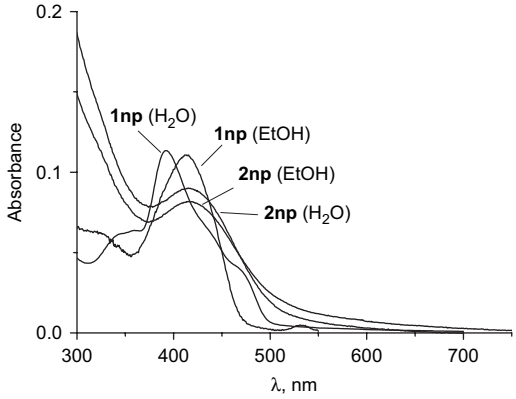

Figure 4. Absorption spectra of 0.2 mg/mL solutions of **1np** and **2np** in water and ethanol at 25 °C. Overall dye concentrations: [**1**]=1.2×10^{-6} M, [**2**]=1.0×10^{-6} M.

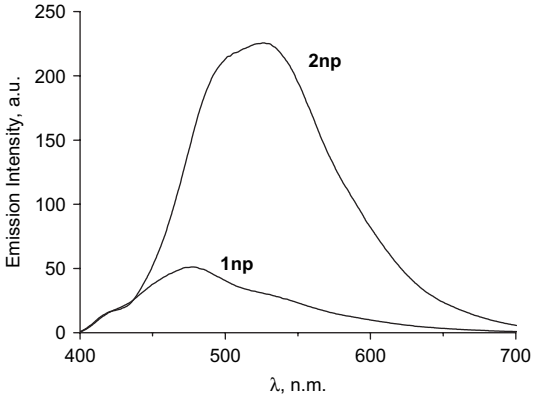

Figure 5. Emission spectra of 0.2 mg/mL ([dye]=1.0×10^{-6} M) solutions of **1np** and **2np** in water. Conditions: λ_{exc}=410 nm, 25 °C.

The emission bands are broad and the positions of the maxima are similar to those recorded for the free dyes in toluene. This indicates that the embedded dyes experience a moderately low polarity environment and that water is excluded by the particle core. Moreover, **2np** shows a much stronger emission (Φ=0.16) than **1np** (Φ=0.06). This result is quite unexpected, since embedding of the more solvent-sensitive dye **2** in the moderately polar nanoparticle environment should result in a lower emission efficiency in the case of **2np** (see Fig. 1). The low emission of **1np** could arise from concentration quenching, due to the formation of nanodomains of aggregated dyes. This phenomenon has been already reported in dye-doped silica nanoparticles:[17] the blue shift of the absorption spectra observed in water suggests that this could be the case also with **1np**.[18]

Besides the speculation on its origin, it is important to note that stronger emission by **2np** is observed also when the particles are excited at 780 nm (Fig. 6A), thus validating the DDNs as two-photon absorbing reporters. Profiles of fluorescence decay show a multiexponential behaviour where a fast component (0.45 ns for **2np** and 0.2 ns for **1np**) and a slower one (2.3 ns for **2np** and 1.6 ns for **1np**) dominate (Fig. 6B). Such complex behaviour is not unprecedented in dye-doped silica nanoparticles and probably arises from the lack of homogeneity of the systems due for instance, to different microenvironments experienced by the dye molecules.[19]

2.3. Cellular uptake

To determine the DDNs' cellular uptake, cells derived from a human oesophageal carcinoma (cell line KYSE-510) were incubated with a suspension of DDNs **1np** and **2np** in culture medium for 120 min and then observed at the epifluorescent microscope (Fig. 7). The DDNs appeared to be rapidly internalized by the cells at a concentration which was not cytotoxic (0.02 mg/mL), as resulted from the cytotoxicity test (see below). The fluorescence images of KYSE-510 cells show significant cellular staining with accumulation of the nanoparticles limited to the cytoplasm, as reported for other silica nanoparticles prepared with the same procedure.[2d]

The cytotoxicity of **1np** and **2np** was determined by using the MTT assay. The results are reported in Figure 8, which shows the amount of cell survival after 120 min of incubation with increasing concentrations of DDNs. Analysis of data reported in Figure 8 reveals that the presence of DDNs slightly affects cell viability up to a 0.02 mg/mL concentration.

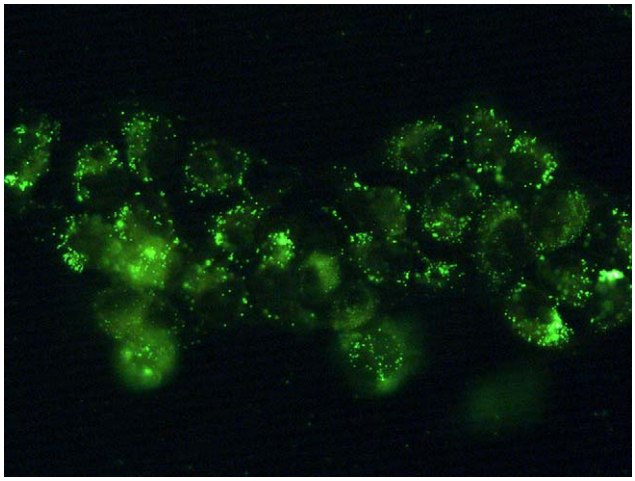

Figure 7. Epifluorescence microscopy showing uptake of **2np** by KYSE-510 cells. Conditions: nanoparticle concentration 0.02 mg/mL ([**2**]=0.1 μM), magnification 400x.

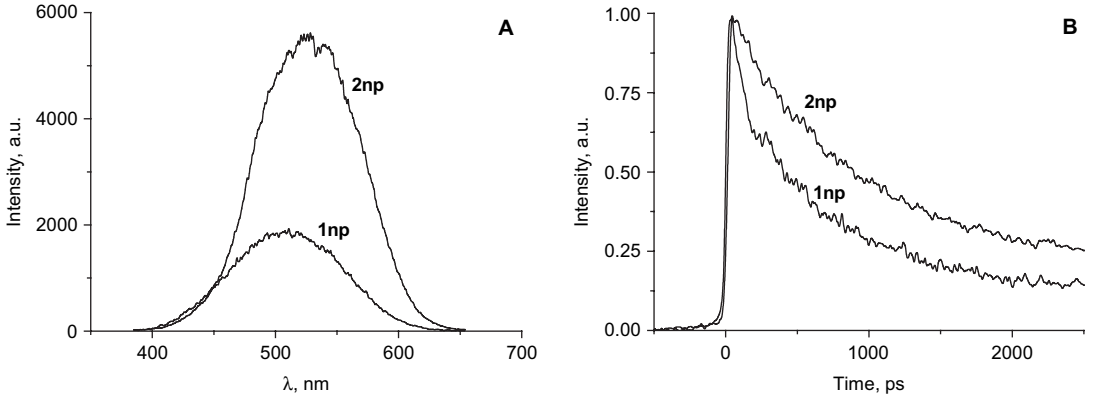

Figure 6. Emission spectra (A) and fluorescence decays (B) of 2.0 mg/mL solutions of dye-doped nanoparticles **1np** and **2np** in water upon two-photon excitation. Emission spectral shapes are affected by the use of an optical filter to cut the laser excitation. Both measurements were performed with the same filter so that the overall peak intensities are comparable. Overall dye concentrations: [**1**]=0.8×10^{-5} M, [**2**]=1.1×10^{-5} M. Conditions: λ_{exc}=780 nm, 25 °C.

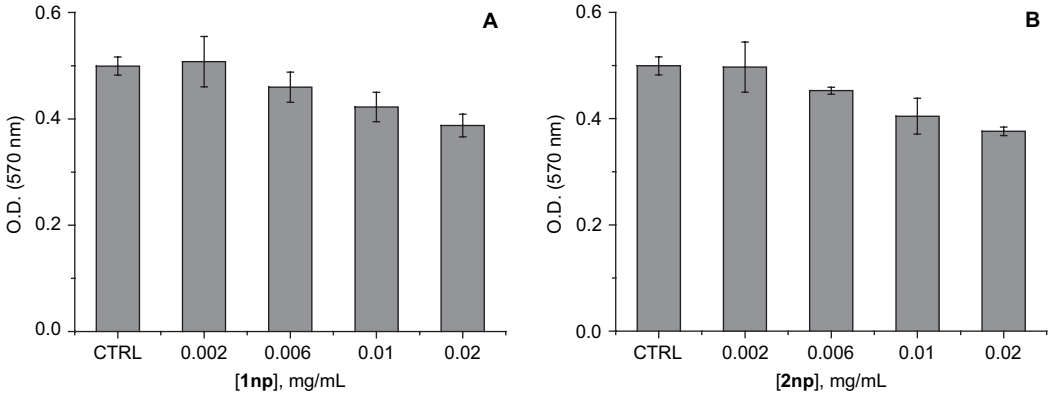

Figure 8. Viability of KISE-510 cells after incubation with **1np** (A) and **2np** (B) for 120 min, expressed as optical density (OD) at 570 nm after MTT treatment. The OD values at 570 nm are the mean of three replicates±standard deviation. CTRL=control.

3. Conclusions

The results obtained in this work indicate that it is possible to embed two-photon absorbing dyes into silica nanoparticles without any chemical modification of the dye structures. New insights have been obtained on the properties and behaviour of such DDNs. The particles are efficiently taken up by cells and localized in the cytoplasm. Fluorescence emission upon 780 nm excitation is observed and the decay profiles witness that the dye molecules embedded in the particles experience dishomogeneous environments. Nanoparticle inclusion has different effects on the emission properties of the embedded dyes, which cannot be easily deduced by their solution behaviour: DDNs doped with the less solvent-sensitive and more strongly emitting dye **1** show a quenched fluorescence emission in water, possibly due to aggregation of the dyes within the particles. To the contrary, **2np** shows a remarkably good emission quantum yield and, as a consequence, reveals to be strong emitting, water soluble, two-photon absorbing reporter that can easily penetrate and stain living cells.

4. Experimental

4.1. General

All commercially available solvents and reagents were used as received without further purification. Preparative column chromatography was carried out on glass columns packed with Macherey-Nagel 60 (70–230 mesh) silica gel. Compound **1**[14] and phosphonate **3**[20] were prepared as described.

Melting points were taken with a Buchi 510 apparatus and are uncorrected. NMR spectra were recorded with a Bruker AC 250F spectrometer. Chemical shifts are reported relative to tetramethylsilane as internal standard. Signals in NMR spectra are reported as follows: s=singlet, d=doublet, m=multiplet, br=broad. ESI-MS mass spectra were obtained with a Navigator ThermoQuest-Finningan mass spectrometer. Elemental analyses were performed by the Microanalysis Laboratory of the Department of Chemical Sciences of the University of Padova.

Transmission Electron Microscopy (TEM) experiments were performed at the Microscopy Facility of the Department of Biology of the University of Padova. TEM images of the particles were obtained with a Fei Tecnai 12 transmission electron microscope operating at 100 keV. Samples for TEM were prepared by spreading a drop of nanoparticle solution in water (~3 mg/mL) onto standard carbon-coated copper grids (200 mesh). Dimensional analysis of nanoparticles from TEM images was made with the *ImageJ* software.[21]

Dynamic Light Scattering measurements were obtained with a Particle Sizing Systems Nicomp Model 370 correlator equipped with a thermostated cell holder and a Spectra Physics Series 2016 Ar laser operating at 488 nm. Hydrodynamic particle diameters were obtained from cumulant fits of the autocorrelation functions at 90° scattering angle.

UV–vis absorption measurements were performed at 25 °C by means of Perkin–Elmer Lambda 16 e 45 spectrophotometers equipped with thermostated cell holders. Quartz cells with optical pathlength of 1 cm were used. Fluorescence spectra were recorded at 25 °C with a Perkin–Elmer LS-55 spectrofluorimeter equipped with a Hamamatsu R928 photomultiplier and thermostated cell holder, quartz cells with optical pathlength of 1 cm were used. Fluorescence quantum yields were determined using Coumarin 153 in ethanol (Φ=0.58) as standard.

Two-photon excitation was performed with a Ti:sapphire femtosecond laser (Spectra-Physics). A 2 mm Schott B18 filter was used to cut the laser excitation. Time resolved measurements were performed with a Hamamatsu streak camera.

4.2. Synthesis of 2

Phosphonate **3** (0.82 g, 2.0 mmol) was dissolved in 50 mL of anhydrous THF and the solution was cooled to 0 °C in an ice bath. 4-(Dimethylamino)benzaldehyde (0.29 g, 1.90 mmol) and NaH (0.13 g, 5.9 mmol) were added and the reaction mixture was stirred overnight under a nitrogen atmosphere (TLC, toluene/ethyl acetate 95:5). The solvent was evaporated and the crude product was purified by flash column chromatography (silica gel, eluent: toluene/ethyl acetate 95:5) and recrystallized from hexane/ethyl acetate to yield 0.46 g (58%) of an orange powder. Mp: 228–230 °C. IR (KBr): 3050–2800 (CH), 2200 (CN), 1607, 1522 (C=C),

1209, 1043, 956 cm^{-1} (CH). ^1H NMR (250 MHz, $CDCl_3$) δ: 7.61–7.56 (m, 5H), 7.47 (d, 2H, J=8.8 Hz), 7.30 (d, 1H, J_{trans}=17.0 Hz), 7.13–7.05 (m, 4H), 6.75 (br s, 2H), 3.94 (s, 3H), 3.92 (s, 3H), 3.01 ppm (s, 6H). ^{13}C NMR (62.9 MHz, $CDCl_3$) δ: 151.95, 151.07, 148.72, 142.56, 132.38, 127.81, 127.12, 126.76, 126.16, 119.21, 109.99, 109.32, 108.44, 56.40, 56.19 ppm. Elemental analysis for $C_{27}H_{26}N_2O_2$ (410.51): calculated (%): C, 79.00; H, 6.38; N, 6.82. Found: C, 78.04; H, 5.98; N, 6.61.

4.3. Preparation of the dye-doped silica nanoparticles (DDNs)

Preparation of nanoparticles containing **1** is reported as an example of general procedure. Particles containing **2** were prepared by following the same procedure with the exception that 20 μL of a 15 mM dye solution in DMF was used.

A 3.0 mM solution of **1** (100 μL) in DMSO, followed by 200 μL of propyltriethoxysilane (PTES), was added to 20 mL of a stirred solution of AOT (0.44 g) and *n*-butanol (800 μM) in water. After 30 min, 10 μL of 3-aminopropyltriethoxysilane (APTES) were added. The reaction mixture was thermostated at 25 °C and vigorously stirred for 16 h. The resulting nanoparticle suspension was diluted to 70 mL with water and transferred into a 75 mL Amicon Ultrafiltration Cell, equipped with a 10-kDa regenerated cellulose membrane and an 800 mL solvent reservoir. The mixture was extensively ultra-filtered under a pressure of 4 bars (about 1600 mL of water were used). The solution obtained was finally filtrated through a 0.45 μm filter membrane. The dye concentrations in the resulting DDN solutions were obtained from their absorbances (**1**: λ_{max}=413 nm, ε=6.9×10^4 M^{-1} cm^{-1}; **2**: λ_{max}=425 nm, ε=7.3×10^4 M^{-1} cm^{-1}).

4.4. Nanoparticle uptake and imaging

The cells KYSE-510 (human oesophageal squamous cell carcinoma) were maintained in RPMI 1640 medium (Invitrogen) supplemented with 10% heat-inactivated foetal bovine serum (FCS, Seromed) in a humidified incubator in an atmosphere of 5% CO_2 in air. For nanoparticle uptake and imaging, the cells were trypsinized, resuspended in fresh medium and seeded in 30-mm culture plates containing a glass cover slip (50×10^3 cells/plate). The next day, the cells were incubated with a suspension of DDNs **1np** and **2np** in RPMI without serum for 120 min and rinsed with PBS. After incubation in complete medium (RPMI 1640 plus FCS) for 1–2 h, the cells were observed by epifluorescent microscopy Leica DMR.

4.5. Cell viability assay

An in vitro MTT based assay kit (Sigma) was used to test the cytotoxicity of **1np** and **2np**. The MTT (3-[4,5-dimethylthiazol-2-yl]2,5-diphenyl tetrazolium bromide) method is designed for determining metabolically active cells on the basis of the reduction of MTT into formazan by mitochondrial dehydrogenases. The formazan crystals are dissolved in acidified isopropanol and the solution is spectrophotometrically measured at 570 nm. The cells were seeded in 96 multiwell-plates (13×10^3 cells/well) and incubated with a suspension of DDNs, as described above. After treatment, MTT solution was added and the cells were incubated following the supplier indications. The optical densities at 570 nm were used to determine the viability of cells after incubation with increasing nanoparticle concentrations.

Acknowledgements

The authors thank Professor Moreno Meneghetti for helpful discussions and Mr. Giuseppe Tognon (CNR-ITB) for kind help with TEM analysis. Financial support for this research has been partly provided by the Ministry of Instruction, University and Research (MIUR contracts PRIN-2004035502, FIRB-RBNE033KMA '*Composti molecolari e materiali ibridi nanostrutturati con proprietà ottiche risonanti e non risonanti per dispositivi fotonici*', FIRB-RBNE01P4JF) and by University of Padova (University Research Project CPDA034893).

References and notes

1. Stöber, W.; Fink, A.; Bohn, E. *J. Colloid Interface Sci.* **1968**, *26*, 62–69.
2. (a) Verhaegh, N. A. M. A.; Van Blaaderen, A. *Langmuir* **1994**, *10*, 1427–1438; (b) Santra, S.; Xu, J.; Wang, K.; Tan, W. *J. Nanosci. Nanotechnol.* **2004**, *4*, 590–599; (c) Lal, M.; Levy, L.; Kim, K. S.; He, G. S.; Wang, X.; Min, Y. H.; Pakatachi, S.; Prasad, P. N. *Chem. Mater.* **2000**, *12*, 2632–2639; (d) Roy, I.; Ohulchanskyy, T. Y.; Pudavar, H. E.; Bergey, E. J.; Oseroff, A. R.; Morgan, J.; Dougherty, T. J.; Prasad, P. N. *J. Am. Chem. Soc.* **2003**, *125*, 7860–7865.
3. Santra, S.; Yang, H.; Dutta, D.; Stanley, J. T.; Holloway, P. H.; Tan, W.; Moudgilb, B. M.; Mericlea, R. A. *Chem. Commun.* **2004**, 2810–2811.
4. (a) Zhao, X.; Tapec-Dytioco, R.; Tan, W. *J. Am. Chem. Soc.* **2003**, *125*, 11474–11475; (b) Wang, L.; Yang, C.; Tan, W. *Nano Lett.* **2005**, *5*, 37–43.
5. Lai, C.-Y.; Trewyn, B. G.; Jeftinija, D. M.; Jeftinija, K.; Xu, S.; Jeftinija, S.; Lin, V. S.-Y. *J. Am. Chem. Soc.* **2003**, *125*, 4451–4459.
6. (a) Radu, D. R.; Lai, C.-Y.; Jeftinija, K.; Rowe, E. W.; Jeftinija, S.; Lin, V. S.-Y. *J. Am. Chem. Soc.* **2004**, *126*, 13216–13217; (b) Roy, I.; Ohulchanskyy, T. Y.; Bharali, D. J.; Pudavar, H. E.; Mistretta, R. A.; Kaur, N.; Prasad, P. N. *Proc. Natl. Acad. Sci. U.S.A.* **2005**, *102*, 279–284.
7. (a) Koo, Y.-E. L.; Cao, Y.; Kopelman, R.; Koo, S. M.; Brasuel, M.; Philbert, M. A. *Anal. Chem.* **2004**, *76*, 2498–2505; (b) Montalti, M.; Prodi, L.; Zaccheroni, N. *J. Mater. Chem.* **2005**, *15*, 2810–2814; (c) Brasola, E.; Mancin, F.; Rampazzo, E.; Tecilla, P.; Tonellato, U. *Chem. Commun.* **2003**, 3026–3027; (d) Rampazzo, E.; Brasola, E.; Marcuz, S.; Mancin, F.; Tecilla, P.; Tonellato, U. *J. Mater. Chem.* **2005**, *15*, 2687–2696; (e) Arduini, M.; Marcuz, S.; Montolli, M.; Rampazzo, E.; Mancin, F.; Gross, S.; Armelao, L.; Tecilla, P.; Tonellato, U. *Langmuir* **2005**, *21*, 9314–9321; (f) Radu, D. R.; Lai, C.-Y.; Wiench, J. W.; Pruski, M.; Lin, V. S.-Y. *J. Am. Chem. Soc.* **2004**, *126*, 1640–1641; (g) Kim, S.; Pudavar, H. E.; Prasad, P. N. *Chem. Commun.* **2006**, 2071–2073.
8. (a) Zipfel, W. R.; Williams, R. M.; Webb, W. W. *Nat. Biotechnol.* **2003**, *21*, 1368–1376; (b) Rudolf, R.; Mongillo, M.; Rizzuto, R.; Pozzan, T. *Nat. Rev. Mol. Cell Biol.* **2003**, *4*, 579–586.

9. (a) Denk, W.; Strickler, J. H.; Webb, W. W. *Science* **1990**, *248*, 73–76; (b) Gura, T. *Science* **1997**, *276*, 1988–1990.
10. (a) Albota, M.; Beljonne, D.; Brédas, J.-L.; Ehrlich, J. E.; Fu, J.-T.; Heikal, A. A.; Hess, S. E.; Kogej, T.; Levin, M. D.; Marder, S. R.; McCord-Maughon, D.; Perry, J. W.; Röckel, H.; Rumi, M.; Subramaniam, G.; Webb, W. W.; Wu, X.-L.; Xu, C. *Science* **1998**, *281*, 1653–1656; (b) Reinhardt, B. A.; Brott, L. L.; Clarson, S. J.; Dillard, A. G.; Bhatt, J. C.; Kannan, R.; Yuan, L.; He, G. S.; Prasad, P. N. *Chem. Mater.* **1998**, *10*, 1863–1874; (c) Mongin, O.; Porrés, L.; Moreaux, L.; Mertz, J.; Blanchard-Desce, M. *Org. Lett.* **2002**, *4*, 719–722.
11. Buck, S. M.; Xu, H.; Brasuel, M.; Philbert, M. A.; Kopelman, R. *Talanta* **2004**, *63*, 41–59.
12. Levy, L.; Sahoo, Y.; Kim, K.-S.; Bergey, E. J.; Prasad, P. N. *Chem. Mater.* **2002**, *12*, 3715–3721.
13. Rumi, M.; Ehrlich, J. E.; Heikal, A. A.; Perry, J. W.; Barlow, S.; Hu, Z.; McCord-Maughon, D.; Parker, T. C.; Röckel, H.; Thayumanavan, S.; Marder, S. R.; Beljonne, D.; Brédas, J.-L. *J. Am. Chem. Soc.* **2000**, *122*, 9500–9510.
14. Nakaya, T.; Imoto, M. *Bull. Chem. Soc. Jpn.* **1966**, *39*, 1547–1551.
15. Woo, H. Y.; Liu, B.; Kohler, B.; Korystov, D.; Mikhailovsky, A.; Bazan, G. C. *J. Am. Chem. Soc.* **2005**, *127*, 14721–14729.
16. On the basis of the particle diameters and the density of amorphous silica (2.2 g/mL) the dye content of a single DDN can be estimated to be about 70 molecules per particle. However, the reliability of such estimation is greatly affected by the difficulty to measure the real particles density.
17. Montalti, M.; Prodi, L.; Zaccheroni, N.; Zattoni, A.; Reschglian, P.; Falini, G. *Langmuir* **2004**, *20*, 2989–2991.
18. The difference between the absorption spectra observed for **1np** in water and ethanol seems to indicate that ethanol can penetrate the particle core and cause disaggregation of the included dyes.
19. Montalti, M.; Prodi, L.; Zaccheroni, N.; Battistini, G.; Marcuz, S.; Mancin, F.; Rampazzo, E.; Tonellato, U. *Langmuir* **2006**, *22*, 5877–5881.
20. Fabbrini, G.; Menna, E.; Maggini, M.; Canazza, A.; Marcolongo, G.; Meneghetti, M. *J. Am. Chem. Soc.* **2004**, *126*, 6238–6239.
21. Rasband, W. S. *ImageJ*; U.S. National Institutes of Health: Bethesda, MD, USA, 1997–2006; http://rsb.info.nih.gov/ij/.